but increase upon folding the metallacyclopentene fragment. The observed differences in activation energies may thus be traced to steric and electronic ground-state stabilization ($\delta x_0 > 0$) or destablization ($\delta x_0 < 0$) rather than to a transition-state effect. Note, however, that (de)stabilization affects the reaction coordinate everywhere except at $x = 0$.

Conclusions. Three general conclusions seem to be worth mentioning:

(1) The empirical correlation between ground-state structure and activation barrier (eq 3) is directly related to a model potential (eq 4) describing the energy profile of a given molecule along its way to the transition state. It follows that the correlation between $\Delta E(x_0)^*$ and x_0 obtained from a series of related molecules provides information on the energy surfaces of individual molecules. Specifically, eq 5 provides force constant information that can be compared to values obtained by independent methods. Here, k is estimated to be $\sim$25 kcal mol^{-1} Å^{-2} (eq 7), which would seem to be reasonable considering the rather long M–C2 distance and the consequent weakness of the bonds. Similar analyses[13] of nondegenerate Ni–O, Ni–N, and C–O bond-breaking reactions yield force constants of $\sim$90, $\sim$120, and $\sim$1000 kcal mol^{-1} Å^{-2}, again in qualitative agreement with vibrational spectroscopic data. Conversely, and probably more important in practice, predictions should be possible on the dependence of reactivity on structure if force constants are known.

(2) The data underlying Figures 4 and 5 represent a quantitative illustration of Hammond's postulate.[10] Contrary to earlier examples of this kind, which dealt with Ni–O, Ni–N,[14] and C–O[15] bond-dissociation reactions, here the transition-state structure is relatively well-defined due to the symmetry of the degenerate reaction. Consequently, the strong dependence of ΔG^* on the distance along the reaction path is relatively well established.

(3) The results described would seem to bear on the mode of action of an efficient catalyst. Not only should it bring reactants together in proper orientation, i.e. convert entropy into binding energy of the precursor complex, but it should also induce deformations of the reactants along the reaction coordinate, i.e. convert binding energy into strain energy localized in the reaction coordinate. Even small structural changes in the substrate will have large effects on reaction rates. Quantitative knowledge of the dependence of structure on changes in bonding and nonbonding interactions is thus a prerequisite for engineering such catalysts. This also points to a need for accurate structural information. Since careful diffraction studies are capable of determining atomic positions with a precision of $\sim$0.002 Å, interesting results can be expected in this direction.

Registry No. Hf3, 80161-03-1; Hf4, 93531-46-5; Hf7, 90751-94-3; Zr1, 84079-50-5; Zr2, 75361-79-4; Zr3, 75361-74-9; Zr4, 75361-78-3; Zr5, 75361-77-2; Zr6, 98357-83-6; Zr7, 75070-70-1; Zr8, 110133-05-6; Zr9, 97391-17-8.

Supplementary Material Available: An appendix describing the data processing, the coordinates used in the factor analysis, and the results obtained from internal coordinates (12 pages). Ordering information is given on any current masthead page.

(13) Bürgi, H.-B.; Dunitz, J. D. *J. Am. Chem. Soc.* **1987**, *109*, 2924-2926.

(14) Schwarzenbach, G.; Bürgi, H.-B.; Jensen, W. P.; Lawrance, G. A.; Mønsted, L.; Sargeson, A. M. *Inorg. Chem.* **1983**, *22*, 4029-4038.

(15) Jones, P. G.; Kirby, A. J. *J. Am. Chem. Soc.* **1984**, *106*, 6207-6212.

Reactions of Fe^{II}nta and Fe^{II}edda with Hydrogen Peroxide

J. D. Rush[†] and W. H. Koppenol*,[†]

Contribution from the Department of Chemistry, University of Maryland Baltimore County, Catonsville, Maryland 21228. *Received March 23, 1987*

Abstract: Reactions of ferrous nitrilotriacetate (nta) and ethylenediamine-*N*,*N*′-diacetate (edda) complexes with hydrogen peroxide at neutral pH in the presence of formate lead to transient intermediates characterized by absorptions near 280 and 400 nm as previously observed for hedta as a ligand. The decomposition of hydrogen peroxide by Fe^{III}nta and -edda leads to ligand destruction, which is not inhibited by formate. During this process a reactive intermediate is scavenged by ABTS [2,2′-azinobis(3-ethyl-2,3-dihydrobenzothiazole-6-sulfonate)] at concentrations of the latter that are much higher than expected if the hydroxyl radical were the reactive intermediate. This intermediate is not scavenged by the bromide ion. These stopped-flow and steady-state experiments give evidence for the following reactions (HL = nta, edda): (a) $HLFe^{II} + H_2O_2 \rightarrow HLFe(H_2O_2)$, (b) $HLFe(H_2O_2) + HLFe^{II} + 2H^+ \rightarrow 2HLFe^{III} + 2H_2O$, (c) $HLFe(H_2O_2) + HCO_2^- \rightarrow L^{\bullet}Fe^{II} + CO_2^{\bullet-} + 2H_2O$, (d) $HLFe(H_2O_2) + H^+ \rightarrow L^+Fe^{II} + 2H_2O$, (e) $HLFe(H_2O_2) + ABTS + 2H^+ \rightarrow HLFe^{III} + ABTS^{\bullet+} + 2H_2O$. Reactions b–e are ascribed to a compound designated as $HLFe(H_2O_2)$ in reaction a, which might be a hypervalent iron complex $HLFe^{IV}(OH^-)_2$ but not a hydroxyl radical. The ability of the $HLFe(H_2O_2)$ complex to oxidize ethanol but not bromide suggests a one-electron reduction potential greater than $E^{\circ\prime}(CH_3{}^{\bullet}CHOH,H^+/CH_3CH_2OH) = 1.2$ V at pH 7 and smaller than $E^{\circ}(Br_2^{\bullet-}/2Br^-) = 1.63$ V.

Superoxide anions are produced in vivo (see below) and dismutate to oxygen and hydrogen peroxide. The one-electron reduction of the latter[1] by adventitious metal ions such as Fe^I and Cu^I is generally thought to produce the reactive hydroxyl radical. This process is considered to cause oxidative damage. In reactions 1–3 RH is a scavenger and HL is a multidentate ligand for iron

$$O_2^{\bullet-} + HLFe^{III} \rightarrow HLFe^{II} + O_2 \quad (1)$$

$$HLFe^{II} + H_2O_2 + H^+ \rightarrow HLFe^{III} + {}^{\bullet}OH + H_2O \quad (2)$$

$$^{\bullet}OH + RH \rightarrow H_2O + R^{\bullet} \quad (3)$$

[†] Present address: Department of Chemistry and Biodynamics Institute, Louisiana State University, Baton Rouge, LA 70803-1804.

0002-7863/88/1510-4957$01.50/0

in which the H denotes a covalently bound hydrogen. The precursor of hydrogen peroxide is the superoxide anion, which is thought to be formed in mitochondria[6] and leucocytes[7] and possibly through dissociation from oxyhemoglobin.[8] A freely diffusing hydroxyl radical, as formed in eq 2, would cause damage throughout the cellular environment that can be prevented by radical scavengers. The mechanism of site-specific damage[4] and the formation of a "crypto-•OH"[9] have been proposed in order to explain the sensitivity of biomolecules to free-radical damage and the failure of common hydroxyl radical scavengers to completely inhibit damage in model systems.[10,11] The effect of ethanol and formate ions on the chain length of hydrogen peroxide decomposition catalyzed by copper(I) and iron(II) complexes, respectively, has been cited previously[12,13] as evidence for the occurrence of higher metal oxidation states in Fenton-like reactions at neutral pH.[14] Higher valent or oxoiron species play a role in reactions of catalase, peroxidases, and, as recently has been shown, cytochrome *c* oxidase.[15,16] Evidence has been obtained for oxygen transfer to Fe^{III}edta in methanol to yield formally FeO^{3+}edta.[17] The 4+ oxidation state can be obtained with simple ligands in aqueous media at alkaline pH.[18] An iron(IV) species is expected to be a strong one-electron oxidizing agent. The reduction potential of the ferryl/ferric edta couple has been estimated theoretically to be in excess of 0.9 V at pH 7.[19] The possibility of an intermediate ferryl species with simple ligands reacting as in eq 4–6 at neutral pH is the subject of this study. Reactions 4–6

$$HLFe^{II} + H_2O_2 \rightarrow HLFe(H_2O_2) \quad (4)$$

$$HLFe(H_2O_2) + RH + H^+ \rightarrow HLFe^{III} + R^\bullet + 2H_2O \quad (5)$$

$$HLFe(H_2O_2) + H^+ \rightarrow L^+Fe^{II} + 2H_2O \quad (6)$$

would lead to damage at or close to the site of metal binding. Various efforts to distinguish between the reactive intermediates formed by reactions 2 and 4 have been made by measuring the rates and determining the products of subsequent reactions with scavengers.[20,21] Although hydroxyl radicals are formed in the reaction of Fe^{II} at low pH,[22-26] results are more ambiguous for complex iron species at higher pH. In previous studies,[26,27] we attempted to resolve this question by measuring the ratio of the rate constant for reaction of the intermediate generated in reaction 4 with organic substrates to the rate constant of the intermediate with the iron(II) poly(amino carboxylate). It was found that *tert*-butyl alcohol and the benzoate anion did not significantly scavenge the intermediate formed in reaction 4 and that the concentration of ethanol necessary to scavenge this intermediate was higher than expected for the hydroxyl radical. The most significant evidence for a non-hydroxyl intermediate capable of oxidizing organic molecules was obtained from the reaction of Fe^{II}hedta (hedta = *N'*-(2-hydroxyethyl)ethylenediamine-*N*,*N*,-*N'*-triacetate) with hydrogen peroxide in the presence of formate ion, which resulted in the formation of a ferrous ligand radical complex. Since hedta is essentially a pentadentate ligand, we extended our studies to the small chelating agents nitrilotriacetate (nta) and ethylenediamine-*N*,*N'*-diacetate (edda), which form strong quadridentate Fe^{II} and Fe^{III} complexes. Stopped-flow reactions and steady-state peroxide decomposition experiments were carried out with ABTS [2,2'-azinobis(3-ethyl-2,3-dihydrobenzothiazole-6-sulfonate)], sodium formate, and ethanol as scavengers. Our results suggest that oxidizing iron intermediates do occur and are responsible for oxidative degradation at the site of iron binding.[28]

Table I. Dependence of the Reactions of Fe^{II}nta and Fe^{II}edda with Hydrogen Peroxide on the Iron(II) Concentration (pH 7.2, 0.0125 M Phosphate, 25 °C)

$[Fe^{II}]$, 10^4 M	k_{obsd}(nta), s^{-1}	k_{obsd}(edda), s^{-1}
1.56	6.5	13.0
3.13	13.0	24.1
6.25	22.2	46.0
12.5	43.0	96.0

Experimental Section

Apparatus and Methods. Kinetic experiments were performed on a stopped-flow apparatus purchased from Kinetic Instruments, Inc. The optical system and data acquisition programs, operating on a Zenith microcomputer, were supplied by On-Line Instruments Systems, Inc. (OLIS). Kinetic data analysis was performed with nonlinear least-squares fitting routines also supplied by OLIS. Solutions to be reacted were kept at 25 °C. For anaerobic experiments solutions were bubbled with nitrogen and transferred to the stopped-flow spectrometer in gas-tight syringes. During one set of experiments, the hydrogen peroxide solution was not deaerated so as to yield a half-air-saturated solution (140 μM[8]). Routine optical spectra were obtained on a Beckman DU7-HS spectrophotometer at ambient temperatures, as were measurements of the ABTS free radical generated in $Fe^{III}HL/H_2O_2$ systems.

Stopped-flow reactions of Fe^{II}edda and Fe^{II}nta complexes with hydrogen peroxide were monitored at wavelengths in the range 260–400 nm, under conditions of excess Fe^{II} complex. The ferrous complexes were prepared by dissolving ferrous ammonium sulfate in a deaerated solution of excess (2:1) ligand. The effective stability constants at pH 7 for the complexes were calculated from data for the equilibria[29] $Fe^{2+} + H'LH \rightleftharpoons FeLH + H'^+$ to be $10^{6.1}$ and 10^7 for H'LH = $ntaH^{2-}$ and $eddaH^-$, respectively. This ensured >95% complexation for most experiments. Solutions of ferric complexes were prepared by oxidizing the ferrous solutions in a stream of air and were kept refrigerated at pH ~5 before use. This procedure results in the formation of at most half as much hydrogen peroxide as there is ferric complex, which is small compared to the amounts of hydrogen peroxide added in the steady-state decomposition experiments (see below). Ferric hydroxide precipitated from

(1) Fenton, H. J. H. *J. Chem. Soc.* **1894**, *65*, 899.
(2) Aust, S. D.; Morehouse, L. A.; Thomas, C. E. *J. Free Radicals Biol. Med.* **1985**, *1*, 3, and references therein.
(3) Winston, G. W.; Feierman, D. E.; Cederbaum, A. I. *Arch. Biochem. Biophys.* **1984**, *232*, 377.
(4) Halliwell, B.; Gutteridge, G. M. J. *Arch. Biochem. Biophys.* **1986**, *246*, 501.
(5) Goldstein, S.; Czapski, G. *J. Free Radicals Biol. Med.* **1986**, *2*, 3, and references therein.
(6) Jamieson, D.; Chance, B.; Cadenas, E.; Boveris, A. *Annu. Rev. Physiol.* **1986**, *48*, 703.
(7) Babior, B. M.; Kipnes, R. S.; Curnutte, J. T. *J. Clin. Invest.* **1974**, *47*, 741.
(8) Koppenol, W. H.; Butler, J. *Adv. Free Radical Biol. Med.* **1985**, *1*, 91.
(9) Elstner, E. F.; Osswald, W.; Konze, J. R. *FEBS Lett.* **1980**, *121*, 219.
(10) Samuni, A.; Aronovitch, J.; Grodinger, D.; Chevion, M.; Czapski, G. *Eur. J. Biochem.* **1983**, *137*, 119.
(11) Winterbourn, C. C.; Sutton, H. C. In *Oxygen Radicals in Chemistry*; Bors, W., Saran, N., Tait, D., Eds.; De Gruyter: New York, 1984; pp 185–191.
(12) Johnson, G. R. A.; Nazhat, N. B.; Saadala-Nazhat, R. A. *J. Chem. Soc., Chem. Commun.* **1985**, 407.
(13) Sutton, H. C.; Winterbourn, C. C. *Arch. Biochem. Biophys.* **1984**, *235*, 106.
(14) Bray, W. C.; Gorin, M. *J. Am. Chem. Soc.* **1932**, *54*, 2124.
(15) Chance, B.; Sies, H.; Boveris, A. *Physiol. Rev.* **1979**, *59*, 527.
(16) Witt, S. N.; Blair, D. F.; Chan, S. I. *J. Biol. Chem.* **1986**, *261*, 8104.
(17) Balasubramanian, P. N.; Bruice, T. C. *J. Am. Chem. Soc.* **1986**, *108*, 5495.
(18) Rush, J. D.; Bielski, B. H. J. *J. Am. Chem. Soc.* **1986**, *108*, 523.
(19) Koppenol, W. H.; Liebman, J. *J. Phys. Chem.* **1984**, *28*, 3643.
(20) Walling, C.; Partch, R. E.; Weill, T. W. *Proc. Natl. Acad. Sci. U.S.A.* **1975**, *72*, 140.
(21) Shiga, T. *J. Phys. Chem.* **1965**, *69*, 3805.
(22) Groves, J. T. In *Metal Ion Activation of Dioxygen*; Spiro, T. G., Ed.; Wiley: New York, 1980; pp 125–162.
(23) Walling, C. *Acc. Chem. Res.* **1975**, 125.
(24) Cahill, A. E.; Taube, H. *J. Am. Chem. Soc.* **1952**, *74*, 2312.
(25) Walling, C.; Cleary, M. *Int. J. Chem. Kinet.* **1977**, *9*, 595.
(26) Rush, J. D.; Koppenol, W. H. *J. Inorg. Biochem.* **1987**, *29*, 199.
(27) Rush, J. D.; Koppenol, W. H. *J. Biol. Chem.* **1986**, *261*, 6730.
(28) Some of these results have been presented at the 194th American Chemical Society National Meeting, New Orleans, August 30th–September 4th, 1987; Abstract INOR 335.
(29) Sillen, L. G.; Martell, A. E. *Spec. Publ.—Chem. Soc.* **1964**, *No. 17*, 507, 519.

Fe^{III}edda solutions, if kept for long periods, possibly because of ligand decomposition. These solutions were therefore prepared freshly. The iron(III) species present at pH ~7 in dilute (3×10^{-4} M) solutions were found to be monomeric by the concentration dependences of their absorption spectra.

The steady-state decomposition of hydrogen peroxide by Fe^{III}edda and Fe^{III}nta was studied at room temperature. Reactants were mixed in 25-mL Erlenmeyer flasks left open to the air. The reactions were initiated by addition of hydrogen peroxide and determined to be complete when the spectrum of H_2O_2 at $\lambda < 260$ nm had disappeared. In experiments in which ABTS was used, the formation of the cation radical was followed spectrophotometrically. The final $ABTS^{\bullet+}$ radical concentration was stable once peroxide decomposition was complete as indicated by a stable absorption at 660 nm. The pH in all experiments was 7.2 ± 0.2.

Simulations of $ABTS^{\bullet+}$ formation were carried out on a Zenith 100 microcomputer by numerically integrating the reactions involved in the iron-catalyzed decomposition of peroxide. The chain carriers in this process, iron(II) complex, superoxide, and the oxidizing intermediate (iron complex or hydroxyl radical), were treated as steady-state quantitites.

Chemicals. Common chemicals (NaCl, NaBr, sodium phosphates, and sodium formate) used in all preparations were Baker Reagents. Nta and edda ligands were from Aldrich. The radical scavenger ABTS was obtained from Sigma. Its green radical cation, $ABTS^{\bullet+}$ is stable in the absence of reducing agents and was monitored by its absorption spectrum near 660 nm ($\epsilon_{660} = 1.4 \times 10^4$ M^{-1} cm^{-1}).[30,31] Hydrogen peroxide stock solutions were prepared from Baker Analyzed Reagent 30% hydrogen peroxide and titrated periodically with potassium permanganate. The water used in all experiments was prepared by reverse osmosis (Osmonics) followed by deionization (MarCor). Nitrogen (Puritan-Bennet) used to remove oxygen was of 99.99% purity.

Results

Kinetics. The oxidations of Fe^{II}edda and Fe^{II}nta by hydrogen peroxide were studied in a phosphate-buffered medium at pH 7.2. The observed rate constants for the reactions were measured over an eightfold range of iron complex concentrations. At pH 7.2 the rate law for iron(III) formation was first order in both reactants for both systems. Second-order rate constants, $k_4(Fe^{II}edda) = 7.8 \times 10^4$ M^{-1} s^{-1} and $k_4(Fe^{II}nta) = 3 \times 10^4$ M^{-1} s^{-1}, were obtained from the rate data summarized in Table I. The overall stoichiometry of the reactions, as determined spectrophotometrically, is consistent with reactions 4 and 7. The oxidizing intermediates of both reactions, whether iron complex (ferryl) or hydroxyl radical, are referred to as $HLFe(H_2O_2)$. The identification of the intermediate as an iron complex required further experiments.

$$HLFe^{II} + H_2O_2 \rightarrow HLFe(H_2O_2) \quad (4)$$

$$HLFe^{II} + HLFe(H_2O_2) \xrightarrow{fast} 2HLFe^{III} \quad (7)$$

Formate Scavenging Dependences. In a previous study,[26] it was found that in the presence of sodium formate the reaction between ferrous hedta and hydrogen peroxide caused the formation of a relatively long-lived radical. The spectrum of this species and the rate constant for its second-order decay were very similar to those of the ligand radical forms of Co^{II}nta and Mn^{II}nta, both of which are formed by the action of hydroxyl radicals, generated by pulse radiolysis, on the respective complexes.[32] By contrast, $^{\bullet}OH$ radicals oxidize iron(II) poly(amino carboxylate) complexes directly to the ferric species.[32] In the presence of excess formate ion, a hydroxyl radical generated by the Fenton reaction would be expected to cause reactions 8 and 9. The carbon dioxide radical anion is a strong reducing agent, $E^{\circ\prime}(CO_2(aq)/CO_2^{\bullet-}(aq)) = 1.84 \pm 0.22$ V.[33]

$$^{\bullet}OH + HCO_2^- \rightarrow H_2O + CO_2^{\bullet-} \quad (8)$$

$$CO_2^- + HLFe^{III} \rightarrow HLFe^{II} + CO_2 \quad (9)$$

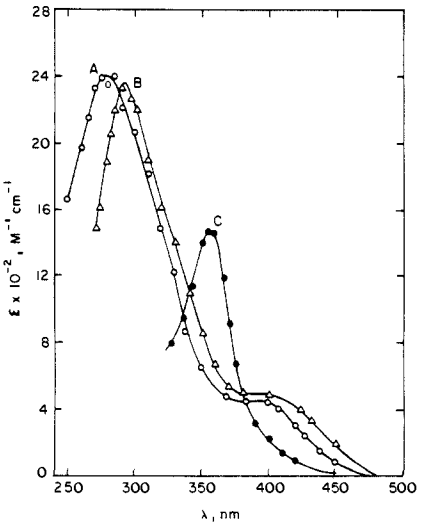

Figure 1. Transient spectra formed by reaction of $HLFe^{II}$ with H_2O_2 in the presence of sodium formate, pH 7.2: (A) assigned to the Fe^{II}edda ligand radical and (B) to the Fe^{II}nta ligand radical; (C) spectrum of Fe^{III}edda–O_2H in a half-air-saturated solution relative to ferric products.

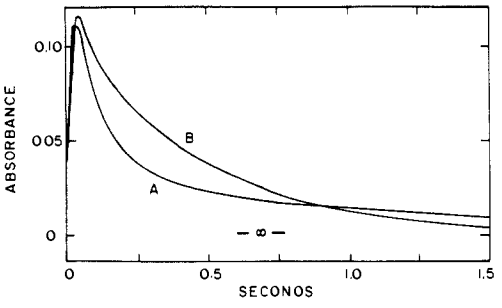

Figure 2. Stopped-flow traces at 320 nm of (A) second-order decay of Fe^{II}edda$^{\bullet}$ radical in deaerated formate solution and (B) first-order decay obtained in the same solution (half-air-saturated, 140 μM O_2). Conditions: 75 μM Fe^{II}edda, 1.5 mM H_2O_2, 25 °C, pH 7.2. Ligand was present in 50% excess.

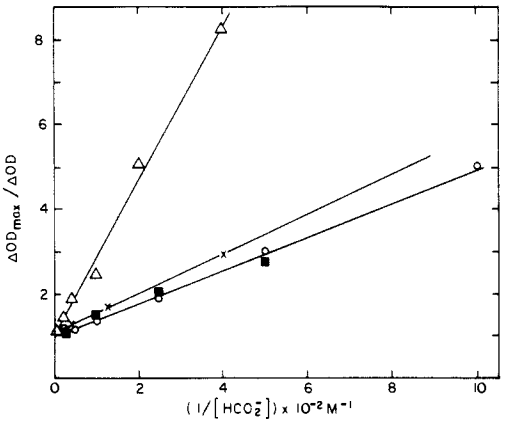

Figure 3. Dependences of the relative intensity of transient spectra ($\Delta OD_{max}/\Delta OD$) on $[HCO_2^-]$: (△) Fe^{II}hedta$^{\bullet}$ radical;[26] (×) Fe^{II}nta$^{\bullet}$ radical; (○) Fe^{II}edda$^{\bullet}$ radical; (■) Fe^{III}edda–O_2H. Conditions were as described for Figure 2.

The reactions of the Fe^{II}edda and Fe^{II}nta complexes (2×10^{-3} M) with H_2O_2 (5×10^{-5} M) were carried out in the presence of sodium formate (5×10^{-4} M ≤ $[HCO_2^-]$ ≤ 0.1 M). The formate/peroxide solutions were deaerated with nitrogen before reaction in the stopped-flow spectrometer. In both cases a transient spectrum, which decayed by second-order kinetics, was observed. The point-by-point spectra of the transients are shown in Figure 1. These spectra are very similar to those of the Fe^{II}hedta ligand radical ($\epsilon_{295} = 2640$, $\epsilon_{420} = 620$ M^{-1} cm^{-1})[26] and the Mn^{II}nta radical.[32] A stopped-flow trace of the formation and second-order

(30) Childs, R. E.; Bardsley, W. G. *Biochem. J.* **1975**, *145*, 93.
(31) Wolfenden, B. S.; Willson, R. L. *J. Chem. Soc., Perkin Trans. 2* **1982**, 805.
(32) Lati, J.; Meyerstein, D. *J. Chem. Soc., Dalton Trans.* **1978**, 1105.
(33) Koppenol, W. H.; Rush, J. D. *J. Phys. Chem.* **1987**, *91*, 4429.

decay of the Fe^{II}edda radical is shown in Figure 2, curve A. The intensity of the transient spectrum increases with $[HCO_2^-]$ and reaches a limiting value from which the extinction coefficients of the transients were calculated. Plots of $\Delta OD_{max}/\Delta OD$ vs $[HCO_2^-]^-$ for the edda, nta, and hedta systems are shown in Figure 3 from which stability constants are derived. The reaction of the oxidizing intermediate with formate ion appears to be accounted for in all three systems by reactions 10–12 (LH = hedta, edda, nta). The data in Figure 3 give K_{10}(edda) = 245 ± 5 M^{-1}, K_{10}(nta) = 185 ± 5 M^{-1}, and K_{10}(hedta) = 47 ± 5 M^{-1}. Second-order rate constants for radical decay are $2k_{12}$(edda) = 1.8×10^5 M^{-1} s^{-1}, $2k_{12}$(nta) = 1.2×10^6 M^{-1} s^{-1}, and, from ref 27, $2k_{12}$(hedta) = 5×10^5 M^{-1} s^{-1}.

$$HLFe(H_2O_2) + HCO_2^- \overset{K_{10}}{\rightleftharpoons} HLFe(H_2O_2)(HCO_2^-) \quad (10)$$

$$HLFe(H_2O_2)(HCO_2^-) \xrightarrow{\text{fast}} L^{\bullet}Fe^{II} + CO_2^{\bullet-} + 2H_2O \quad (11)$$

$$2L^{\bullet}Fe^{II} \rightarrow \text{dimerization/disproportionation} \quad (12)$$

The ligand radical complex is most likely formed by abstraction of a methylene proton from the ligand and as such is reactive toward oxygen. The reactions of many carbon-centered radicals with oxygen to form organic peroxyl radicals occur with rate constants on the order of 10^8 M^{-1} s^{-1}. In half-air-saturated solutions, the ligand radical complex Fe^{II}edda$^{\bullet}$ is converted to a species decaying by first-order kinetics (Figure 2, trace B) to an iron(III) species. The difference spectrum of the transient product of reaction 13 relative to the products of reaction 14 is shown in Figure 1, spectrum C. In addition to reactions 10–12, reactions 13–16 also occur in oxygenated solutions. The rate constant for

$$Fe^{II}edda^{\bullet} + O_2 + H^+ \xrightarrow{\sim 10^8\ M^{-1}\ s^{-1}} Fe^{III}edda\text{–}O_2H \quad (13)$$

$$Fe^{III}edda\text{–}O_2H \xrightarrow{1.5\ s^{-1}} \text{ferric decompn products} \quad (14)$$

$$CO_2^{\bullet-} + O_2 \xrightarrow{2.4 \times 10^9\ M^{-1}\ s^{-1}} CO_2 + O_2^{\bullet-} \quad (15)$$

$$O_2^{\bullet-} + Fe^{II}edda + 2H^+ \xrightarrow{\sim 10^8\ M^{-1}\ s^{-1}} Fe^{III}edda + H_2O_2 \quad (16)$$

reaction 15 is from ref 34, and that for reaction 16 is considered similar to the oxidation of Mn^{II}nta by superoxide.[32] Overall, the yield of Fe^{III} is considerably increased due to entrainment of oxygen. That the transient spectrum attributed to Fe^{III}edda–O_2H derived from the Fe^{II}edda$^{\bullet}$ radical is evident from the fact that the formate dependence of its spectral intensity (Figure 3) is the same as that of the Fe^{II}edda$^{\bullet}$ radical.

The above reactions appear to give evidence that the reaction between simple ferrous complexes and hydrogen peroxide gives rise to an iron species capable of oxidizing a simple carbon compound. Ethanol scavenges the intermediates of the nta, edda, and hedta systems but does not give rise to the characteristic transients due to the formate ion although the Gibbs energies at pH 7 for one-electron oxidation of formate, $E^{\circ\prime}(CO_2^{\bullet-}, H^+/HCO_2^{\bullet-})$ = 1.1 V, are comparable to the formation of the α-carbon radical from a corresponding alcohol; $E^{\circ\prime}(CH_2OH,H^+/CH_3OH)$ = 1.2 V.[33] It would seem that formate, an efficient hydroxyl radical scavenger, does not prevent the destruction of the ligand in a site-specific process.

Decomposition of H_2O_2 by Fe^{III}nta and Fe^{III}edda. The decomposition of hydrogen peroxide by ferric edta is known to cause substantial degradation of the ligand.[35] However, since the hydroxyl radical reacts relatively slowly with hydrogen peroxide, $k(H_2O_2 + {}^{\bullet}OH) = 2 \times 10^7$ M^{-1} s^{-1},[36] it is difficult to distinguish site damage from reaction of hydroxyl radicals with excess ferric complex, $k(Fe^{III}edta + {}^{\bullet}OH) = 5 \times 10^8$ M^{-1} s^{-1}.[37] In order to measure damage at an iron binding site, dilute aerated solutions of hydrogen peroxide, buffered with 25 mM sodium or potassium phosphate near pH 7, were decomposed by 3.2 mM ferric nta or edda. These reactions were carried out in the presence and absence of sodium formate (0.1 M) and with varying hydrogen peroxide concentrations. The degree of ligand decomposition was measured qualitatively by the decrease in the absorption spectrum of the complex. Parts A and B of Figure 4 show the changes in the absorption spectra after hydrogen peroxide concentrations of 2–100 mM were completely decomposed by Fe^{III}nta and Fe^{III}edda, respectively. Concentrations of hydrogen peroxide below 10 mM decomposed within a few minutes while the highest concentrations, particularly with Fe^{III}edda, required at least 24 h due to progressive inactivation of the iron complex. Final solution spectra, including that of a blank, were measured after ~24 h. The data for solutions containing formate (Figure 4) and those without were not significantly different.

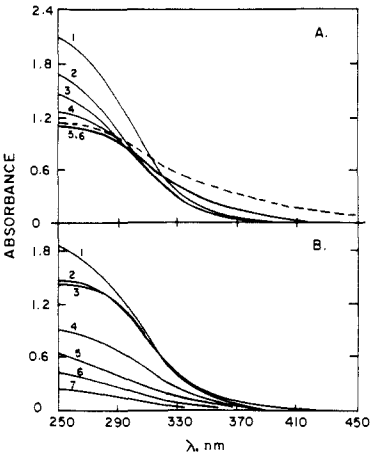

Figure 4. Absorbance changes in Fe^{III}nta (A) and Fe^{III}edda (B) solutions after peroxide decomposition in 0.1 M formate, 3.2×10^{-4} M $HLFe^{III}$, and 6.4×10^{-4} M LH. A: $[H_2O_2]$, M = 0 (1); 0.0125 (2); 0.025 (3); 0.05 (4); 0.1 (5); 0.2 (6). The dashed line is the spectrum of a nta:Fe^{III} = 1:2 solution. B: $[H_2O_2]$, M = 0 (1); 0.0025 (2); 0.005 (3); 0.01 (4); 0.015 (5); 0.025 (6); 0.05 (7). The solutions numbered 4–7 contained ferric precipitates.

The changes in the absorption spectra are due to progressive oxidation of the ligands and subsequent polymerization of the ferric species. This process decreases the rate of further peroxide decomposition. The final spectrum of the Fe^{III}nta system that contained 50 mM hydrogen peroxide at the start was essentially reproduced by preparing a solution without hydrogen peroxide in which the ligand to metal ratio was 1:2. This indicates a predominance of polymers in the system. Smaller ratios resulted in precipitation of polymeric iron. Regeneration of the original spectrum with an excess of added nta required heating of the solution for several minutes to dissociate these polymers. Solutions of the edda complex, which contained in excess of 5 mM hydrogen peroxide, showed visible precipitates after several hours and a cessation of peroxide decomposition. In the absence of peroxide, both complexes were stable for the duration of these experiments.

The chain decomposition of peroxide by ferric complexes usually involves the processes

$$HLFe^{III} + H_2O_2 \rightarrow HLFe^{II} + O_2^- + 2H^+ \quad (17)$$

$$O_2^{\bullet-} + HLFe^{III} \rightarrow HLFe^{II} + O_2 \quad (1)$$

$$HLFe^{II} + H_2O_2 \rightarrow HLFe(H_2O_2) \quad (4)$$

$$HLFe^{III} + {}^{\bullet}OH + OH^- \quad (2)$$

The formate anion is oxidized by products of reactions 2 or 4 to form $CO_2^{\bullet-}$, which also propagates the chain. The oxidation of the organic ligands even in the presence of excess formate is inconsistent with the direct formation of the hydroxyl radical in

(34) Adams, G. E.; Willson, R. L. *Trans. Faraday Soc.* **1969**, 2981.
(35) Francis, K. C.; Cummins, D.; Oakes, J. *J. Chem. Soc., Dalton Trans.* **1985**, 493.
(36) Farhataziz; Ross, A. B. *Natl. Stand. Ref. Data Ser. (U.S., Natl. Bur. Stand.)* **1977**, *59*.
(37) Kundu, K. P.; Matsuura, N. *Int. J. Radiat. Phys. Chem.* **1971**, *3*, 1.

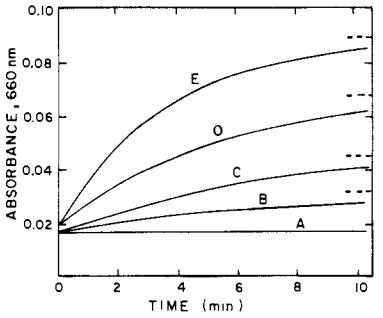

Figure 5. Formation of $ABTS^{\bullet+}$ monitored at 660 nm as a function of time at varying hydrogen peroxide concentrations: $[Fe^{III}edda] = 2.8 \times 10^{-4}$ M, $[ABTS] = 1 \times 10^{-3}$ M. $[H_2O_2] = 0$ (trace A), 3.5×10^{-4} M (trace B), 7×10^{-4} M (trace C), 1.4×10^{-3} M (trace D), and 1.4×10^{-3} M (trace E).

reaction 4, which would be scavenged completely by HCO_2^-; $k_8 = 3 \times 10^9$ M^{-1} s^{-1}.[36] However, reactions 13 and 14 can account for the failure of formate to protect the organic binding site of the iron.

In the absence of formate, ligand degradation through site oxidation or hydroxyl scavenging cannot be distinguished. Though measurable spectral changes required peroxide in excess, this cannot be interpreted as a lack of efficiency in binding-site oxidation. The spectral measurement of ligand oxidation is qualitative, and the edda and nta ligands, being polydentate, are likely to require several moles of hydrogen peroxide per complex before ligand oxidation is extensive enough to result in loss of iron and to cause significant spectral changes.

Scavenging Oxidizing Intermediates with ABTS. As described above, the formate ion reacts with ferryl, or $HLFe(H_2O_2)$, in a manner that may not be characteristic of other organic molecules and leaves open the question of whether the hydroxyl radical may be the oxidant in other cases. The free-radical scavenger ABTS was used as a probe of the oxidizing species that is generated in steady-state systems. The product of its reaction with oxidizing radicals such as $^{\bullet}OH$, $Br_2^{\bullet-}$, $(SCN)_2^{\bullet-}$,[31] or ferryl porphyrins[30,38] is the green cation radical $ABTS^{\bullet+}$, which absorbs at 660 nm. As a scavenger in a $Fe^{III}edda/H_2O_2$ solution, $ABTS^{\bullet+}$ may be formed by either reaction 18 or 20 in competition with reactions 19 and 21, respectively. Rate constants for reactions 18 and 19 are

$$HLFe(H_2O_2) + ABTS + 2H^+ \rightarrow HLFe^{III} + ABTS^+ + 2H_2O \quad (18)$$

$$HLFe(H_2O_2) + H^+ \rightarrow L^+Fe^{II} + 2H_2O \quad (19)$$

$$^{\bullet}OH + ABTS + H^+ \rightarrow ABTS^{\bullet+} + H_2O \quad (20)$$

$$^{\bullet}OH + HLFe^{III} \rightarrow L^+Fe^{II} + H_2O \quad (21)$$

unknown but $k_{20} = 1.2 \times 10^{10}$ M^{-1} s^{-1} [31] and $k_{21} = 10^9$ M^{-1} s^{-1}, analogous to the reaction of $Fe^{III}edta$ with $^{\bullet}OH$.[37] In the presence of excess bromide ion, hydroxyl radicals, if not ferryl, will form the bromine radical, Br_2^-, which also oxidizes ABTS to $ABTS^{\bullet+}$ ($k = 2 \times 10^9$ M^{-1} s^{-1}) with 100% efficiency compared to 58% for reaction 20.[31]

The reduction potential $E°(2Br_2^{\bullet-}/Br^-) = 1.63$ V[39] is significantly higher than that of the $CO_2^{\bullet-}/HCO_2^-$ couple. The selectivity and efficiency of the intermediate formed in reaction 4 toward ABTS in the presence of bromide or formate may therefore be a criterion of whether the intermediate is the hydroxyl radical or an iron complex.

Total amounts of $ABTS^{\bullet+}$ formed are expected to depend on the scavenging rates of reaction 18 or 20, the amount of hydrogen peroxide decomposed by reactions 2 or 4 relative to the initiation step (chain length), and the rates at which $ABTS^{\bullet+}$ is reduced by $Fe^{II}edda$ and superoxide (reaction 17), which are present in steady-state amounts during peroxide decomposition. Generation of $ABTS^{\bullet+}$ in a steady-state system was modeled by computer for systems consisting of reaction 4, 1, 17, 18, and 19 and for reactions 2, 1, 17, 20, and 21. For the purpose of simulation, it was assumed that $k(O_2^- + ABTS^+) = 10^{10}$ M^{-1} s^{-1} and $k_1 = 1 \times 10^7$ M^{-1} s^{-1} by analogy to the manganic complexes.[40] The reduction of $ABTS^{\bullet+}$ by $HLFe^{II}$ was neglected.

Experimentally, the formation of $ABTS^{\bullet+}$ during the decomposition of hydrogen peroxide by $Fe^{III}edda$ was monitored at 660 nm. The approach of the absorbance to a limiting value was approximately exponential. The final concentration, $[ABTS^{\bullet+}]_f$, and the initial rate of formation, $\Delta[ABTS^{\bullet+}]/\Delta t$, were dependent on initial concentrations of $Fe^{III}edda$, H_2O_2, and ABTS. Amounts of $ABTS^+$ formed as a function of time at varying initial hydrogen peroxide concentrations, $[H_2O_2]_0$, are shown in Figure 5. Data in Table II for hydrogen peroxide and $Fe^{III}edda$ dependences are consistent with an initiation by reaction 17. Though peroxide dependences are direct, the more complex $Fe^{III}edda$ dependence may reflect competition between the reactions of superoxide with $Fe^{III}edda$ and with $ABTS^{\bullet+}$, resulting in greater $[ABTS^{\bullet+}]_f$ as $[Fe^{III}edda]_0$ increases. These general characteristics were successfully simulated by the computer model using either system of equations. $ABTS^{\bullet+}$ yields predicted by the models and experimental yields were of the same order of 5–50 μM. The models predicted that $[ABTS^{\bullet+}]$ continues to increase as long as hydrogen peroxide is present in the system.

The dependences of $[ABTS^{\bullet+}]_f$ on $[ABTS]_0$ in $Fe^{III}edda$ and $Fe^{III}nta$ solutions are shown in Figures 6 and 7. Both show continuing ABTS scavenging and inhibition of peroxide decomposition at ABTS concentrations up to 0.01 M. Figure 8 shows simulations of $ABTS^{\bullet+}$ yields in systems where hydroxyl radical is the oxidant (curve D) and for three systems in which a "ferryl"

Table II. Peroxide and Iron(III) Dependences of the Initial Rates of Formation of the $ABTS^{\bullet+}$ Cation Radical during the $Fe^{III}edda$-Catalyzed Decomposition of Hydrogen Peroxide ([ABTS] = 1×10^{-3} M, 5×10^{-3} M Phosphate Buffer, pH 7.2)

$[H_2O_2]$,[a] 10^{-4} M	$d[ABTS^{\bullet+}]/dt$ ($t = 0$), μM/s	total $[ABTS^{\bullet+}]$, μM
3.5	0.01	0.7
7.0	0.02	1.7
14.0	0.04	2.8
27.0	0.08	5.0
$[Fe^{III}edda]$,[b] 10^5 M	$d[ABTS^{\bullet+}]/dt$ ($t = 0$), μM/s	total $[ABTS^{\bullet+}]$, μM
7.0	0.37	2.3
14.0	0.06	2.7
28.0	0.08	5.0

[a] $[Fe^{III}edda] = 2.8 \times 10^{-4}$ M. [b] $[H_2O_2] = 2.7 \times 10^{-3}$ M.

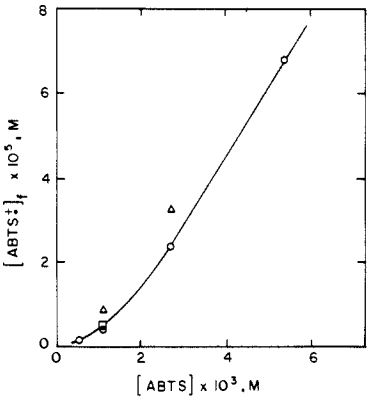

Figure 6. Scavenging of $Fe(H_2O_2)edda$ by ABTS: (○) limiting amounts of $ABTS^{\bullet+}$ in solutions of $[Fe^{III}edda] = 2.2 \times 10^{-4}$ M, $[H_2O_2] = 2.2 \times 10^{-3}$ M, 0.005 M phosphate, pH 7.2, as a function of [ABTS]; (△) with 0.1 M bromide; (□) 0.1 M chloride.

(38) Zipplies, M. R.; Lee, W. A.; Bruice, T. C. *J. Am. Chem. Soc.* **1986**, *108*, 4433.
(39) Schwarz, H. A.; Dodson, R. W. *J. Phys. Chem.* **1984**, *88*, 3643.
(40) Koppenol, W. H.; Levine, F.; Hatmaker, T. L.; Epp, J.; Rush, J. D. *Arch. Biochem. Biophys.* **1986**, *251*, 594.

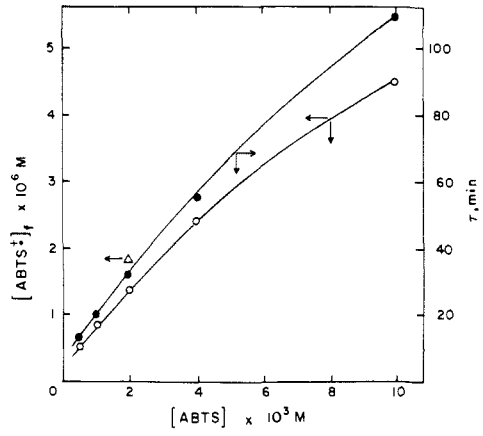

Figure 7. Scavenging of $Fe(H_2O_2)$nta by ABTS and dependence of $[ABTS^{\bullet+}]_f$ and the time constant for its formation (τ = half-life) on [ABTS] in $Fe^{III}nta(H_2O_2)$ solutions: (Δ) $[ABTS^+]_f$ with 0.1 M bromide added. All solutions contained 2.4×10^{-4} M Fe^{III}nta and 1.6×10^{-3} M H_2O_2 in 0.0125 M phosphate, pH 7.2.

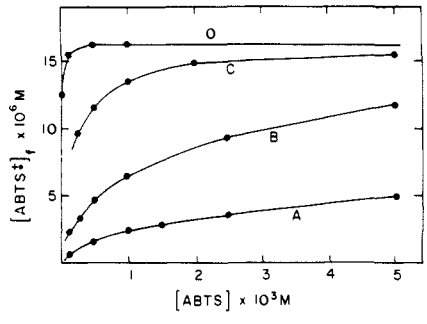

Figure 8. Computed $[ABTS^{\bullet+}]_f$ in simulated peroxide decomposition as a function of initial [ABTS] with $[HLFe^{III}] = 5 \times 10^{-4}$ M and $[H_2O_2] = 3 \times 10^{-4}$ M. The rate of ferryl decomposition k_{19} was taken as 10^3 s^{-1} and k_{18} as 10^4 M^{-1} s^{-1} for curve A, 10^5 M^{-1} s^{-1} for curve B, and 10^6 M^{-1} s^{-1} for curve C. Curve D is calculated for a system in which hydroxyl radical is the oxidizing intermediate.

transient oxidizes ABTS at different rates in competition with oxidation of its binding site (curves A–C). The experimental scavenging is clearly inconsistent with curve D, which requires scavenging and inhibition to reach a maximum at an $ABTS^{\bullet+}$ concentration of approximately 10^{-4} M. Figure 7 is qualitatively similar to curve A in Figure 8, and Figure 6 also shows an increase in $[ABTS^{\bullet+}]$ at $[ABTS]_0 \gg 10^{-4}$ M. The effect of added bromide upon $[ABTS^+]_f$ also suggests that hydroxyl radicals are not the primary oxidants. As shown in Figures 6 and 7, the addition of 0.1 M Br^-, sufficient to scavenge any hydroxyl radicals formed, to the reactant solutions causes some increase in $[ABTS^+]_f$, but this is much less than the maximum values of $[ABTS^+]_f$ obtained; the effect becomes less significant as $[ABTS]_0$ is increased. This shows that little or no $ABTS^+$ is formed through the intermediacy of $Br_2^{\bullet-}$ or $^{\bullet}OH$ at higher [ABTS] and that a hypervalent iron species is the primary oxidant. Chloride ions had negligible effect on $ABTS^{\bullet+}$ yields.

ABTS Scavenging in the Presence of Formate Ion. The effect of formate ion on the yield of the ABTS cation radical in $Fe^{III}edda/H_2O_2$ solutions was measured to determine if formate is oxidized to the $CO_2^{\bullet-}$ radical. This radical propagates the chain decomposition of hydrogen peroxide, and it can be shown by steady-state analysis that the chain length is expected to depend on $[HCO_2^-]^{1/2}$ in this and smaller systems.[13,41] Simple competition between reactions 10 and 18 would yield a dependence of $[ABTS^{\bullet+}]_f$ proportional to $x/(1 + x)$ where $x = k_{18}[ABTS]/k_{10}[HCO_2^-]$. However, the fraction of peroxide decomposed by processes that form $Fe(H_2O_2)$edda is proportional to the chain length, n, and therefore $[ABTS^{\bullet+}]_f$ is proportional to $nx/(1 + nx)$.

(41) Goldstein, S.; Czapski, G. *J. Free Radicals Biol. Med.* **1985**, *1*, 281.

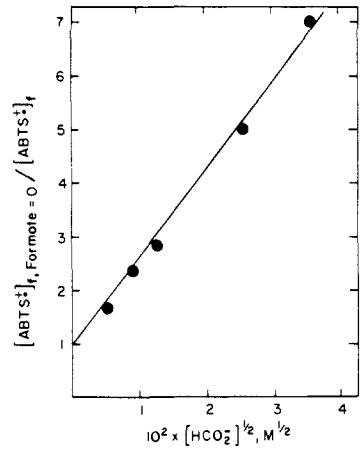

Figure 9. Yields of $[ABTS^{\bullet+}]_f$ relative to $[ABTS^{\bullet+}]_f$ in the absence of formate as a function of formate concentration in a $Fe^{III}edda/H_2O_2$/ABTS solution: [ABTS] = 10^{-3} M, $[Fe^{III}edda] = 2.7 \times 10^{-4}$ M, $[H_2O_2] = 2.7 \times 10^{-3}$ M.

Scheme I

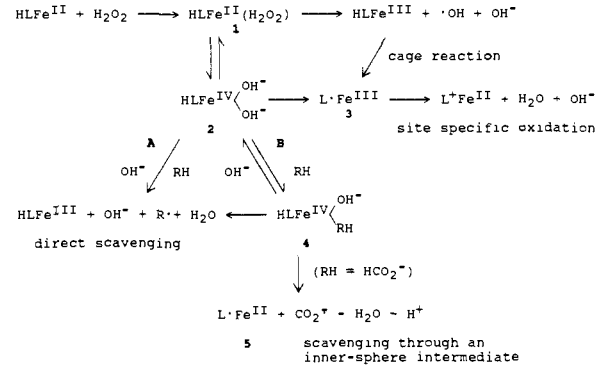

If [ABTS] is constant and unknown rate constants, etc., are eliminated, the following relationship is obtained:

$$[ABTS^{\bullet+}]_f \approx [HCO_2^-]^{-1/2}/(1 + [HCO_2^-]^{-1/2})$$

Experimentally, this dependence is observed as shown by the data in Figure 9. This result supports our formulation of reaction 11 and shows that the inability of formate ion to protect the iron binding site in steady-state decomposition experiments is not due to the failure of formate to scavenge the oxidizing intermediate in the $Fe^{III}edda/H_2O_2$ system.

Discussion

Hydrogen peroxide reacts with Fe^{II}nta and Fe^{II}edda complexes near physiological pH to form an intermediate iron complex, compound **1** or **2** in Scheme I, which is capable of rapidly oxidizing simple organic scavengers in competition with its own decay by oxidation of the ligand. Some formation of the hydroxyl radical cannot be excluded, but it appears to be a minor development under the experimental conditions employed in this study. The decomposition of hydrogen peroxide by Fe(nta) and Fe(edda) complexes is only slightly inhibited by addition of bromide ions, and this in turn causes only a small increase in the amount of $ABTS^+$, which is again inconsistent with the production of hydroxyl radicals as chain carriers. In studies of hydrogen peroxide decomposition by Fe(edta),[42] the inhibition by organic scavengers was generally compatible with the formation of hydroxyl radicals. For edta, dtpa, and hedta complexes of iron we have found that many common scavengers such as ethanol and mannitol are oxidized in a manner that is virtually indistinguishable from their reaction with the hydroxyl radical in that these reactions yield initially a ferric complex and an organic radical.[26] The particular

(42) Walling, C.; Partch, R. E.; Weil, T. *Proc. Natl. Acad. Sci. U.S.A.* **1975**, *72*, 140.

reaction of formate with $HLFe(H_2O_2)$ that leads to a ligand radical, $^{\bullet}LFe^{II}$ (pathway **B** in Scheme I), indicates that in spite of these similarities oxidation occurs via an iron-centered species when hedta, nta, and edda serve as chelating agents.

The pathways in Scheme I can be compared energetically and kinetically. An inner-sphere reaction between hydrogen peroxide and the ferrous complex is postulated. The initial adduct, **1**, might rearrange to an iron(IV) species, **2**, or decompose to the Fenton products, $HLFe^{III}$, and the hydroxyl radical, as shown at the top of Scheme I. An alternative to **2** is a ferryl complex, $HLFeO^{2+}$. However, the presence of d electrons may prevent effective $\pi p-\pi d$ back-bonding as found in such compounds as vanadyl. The energetics of hydroxyl radical formation are favorable by about 5 kcal based on an estimated reduction potential of 0.1 V (vs NHE) of the iron(III)/iron(II) complexes and 0.32 V for $E^{\circ\prime}(H_2O_2, H^+/{}^{\bullet}OH, H_2O)$ at neutral pH.[18] The energetics of iron(IV) formation may be judged to be energetically—if not always kinetically—more favorable since the reaction of the conjugate base of the hydroxyl radical, O^-, with $Fe(OH)_4^-$ yields an iron(IV) complex. This situation is likely to be reversed under very acidic conditions. At pH 7 we estimate $E^{\circ\prime}[HLFe^{IV}(OH^-)_2, H^+/HLFe^{III}OH^-, H_2O]$ to be between 1.2 and 1.6 V (this paper), and $E^{\circ}({}^{\bullet}OH/OH^-)$ is 1.9 V.[39,43] Neglecting the favorable association between the hydroxide anion and the Fe^{IV} complex, one estimates that the formation of the Fe^{IV} species (**2**) is favorable by 7–16 kcal relative to Fe^{III} complex and $^{\bullet}OH$ and by 12–21 kcal relative to $HLFe^{II}$ and hydrogen peroxide. In either pathway only one rate-determining process will be observed kinetically since formation of the oxidizing species is rate limiting. This species then undergoes rapid further reactions, which may, in some cases, permit speculation about its identification.

If an oxidizing iron system is formed, two modes of reaction with scavengers might be postulated. In an outer-sphere process (path A) reactions with organic scavengers yield typical hydrogen-abstraction products ($R^{\bullet}$) and iron(III), whereas if substitution into the coordination sphere of iron precedes oxidation (path B), more complex processes are possible. The accessibility of path B should depend on the degree of iron chelation as well as the ligating properties of the scavenger. In the case of the scavenger formate, the association constant with the intermediate (K_{10}) decreases with increasing chelation of the iron complex, indicating that its site of attack is the iron center rather than the ligand.

The overall process, in which the formate ion is oxidized to $CO_2^{\bullet-}$ and a ferrous ligand radical, **5**, is formed, is thermodynamically possible if the reduction potential of the ligand radical $[E^{\circ\prime}(L^{\bullet},H^+/HL)]$ is about that of the ethanol radical.[26] Since iron(III) formation is energetically more favored, the particular products of formate scavenging must be determined by a complex process within the complex of iron(IV) with scavenger. Not much is known about the structure of aqueous iron(IV) complexes with the exception of porphyrins. This class of compounds is a poor model for the amino polycarboxylate complexes employed in this study. The nta and edda ligands are sufficiently flexible as not to impose steric limitations on iron-centered processes. Two modes of attack by the iron complex seem possible: (i) direct attack by a oxygen coordinated to the iron in which this oxygen behaves as a hydroxyl (or O^-) radical in its oxidizing properties (path A) or (ii) attack by a nucleophile at the iron in which the bond between iron and its oxo ligand may be labilized in favor of a bond between iron and the nucleophile (path B, compound **4**). This latter sequence is illustrated, in which the oxo ligand of iron(IV) is shown (**6**) as stabilized in interactions with an amine ligand analogous to that in ferric porphyrin *N*-oxides.[44] The particular structure of the formate ion permits interaction between its

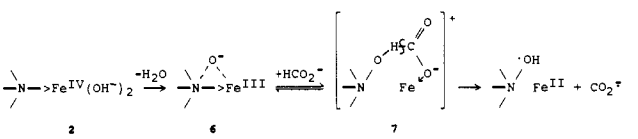

2 **6** **7**

carboxylate group and iron in the transition state (**7**), followed by hydrogen abstraction from its carbon atom. Since formate labilizes the Fe–O bond, the interaction with nitrogen is favored and permits thereby simultaneous ligand and substrate oxidation. The nitrogen radical thus formed, which is equivalent to the hydroxyl radical adduct of an amine, may rearrange to a carbon radical, yielding the spectroscopically observed product **5**. In contrast, ethanol is not expected to replace the hydroxide anion or water bound to iron, and electron transfer will take place according to path A in Scheme I. While speculative, this mechanism may also describe a mode of ligand oxidation that can occur spontaneously when no scavengers are present such as during the degradation of the ferric complexes by hydrogen peroxide.

The biologically damaging effect of iron as a Fenton catalyst has been discussed by Halliwell and Gutteridge.[4] As reviewed, a number of physiological and artificial ligands have been investigated to assess these harmful reactions. Edda, nta, and hedta have donor atoms similar to those found for the systems described above. It seems unlikely that in a biological milieu binding sites are available for adventitious metal ions that completely encapsulate the metal,[45] i.e. that allow 6- or 7-coordinate complexes to be formed. It might therefore be possible that in such a milieu higher oxidation states of iron are formed similar to those described in the present study, although the concentrations of iron and hydrogen peroxide employed are much higher than found in vivo. In the absence of scavengers such higher oxidation states would lead to ligand degradation, or site-specific damage rather than release of hydroxyl radicals.

Note Added in Proof. Goldstein et al.[46] have shown that the carbon dioxide radical anion, $CO_2^{\bullet-}$, reacts with Fe^{II}nta and Fe^{II}hedta to form an intermediate with a spectrum that, above 320 nm, is nearly identical with that reported in Figure 1. The $CO_2^{\bullet-}$ radical is believed to form a σ-bond with Fe^{II}. To determine whether our intermediate is a ligand radical, $^{\bullet}Fe^{II}$, as postulated, or $Fe^{II}CO_2^{\bullet-}$, as suggested by Goldstein et al., we added cobalt(III) hexaammine as a $CO_2^{\bullet-}$ scavenger to final concentrations of 0.5 and 2 mM. The concentrations of Fe^{II}edda, hydrogen peroxide, and sodium formate were 2, 0.1, and 100 mM, respectively. Under these conditions cobalt(III) hexaammine reduced the intensity of the transient's spectrum by approximately 50% without affecting the second-order decay rate of the remainder. No signals were observed in flow ESR experiments with Fe^{II}hedta, hydrogen peroxide, and sodium formate (but no cobalt(III) hexaammine), which indicates that both $L^{\bullet}$ and $CO_2^{\bullet-}$ either are bonded to the ferrous ion or otherwise have signals greatly broadened by its close presence. We conclude that $^{\bullet}LFe^{II}$ and $Fe^{II}CO_2^{\bullet-}$ have absorption spectra that are nearly identical and that some of the absorption shown in Figure 1 is due to $Fe^{II}CO_2^{\bullet-}$. The formation of a ligand radical is also in line with the observations made in the presence of oxygen.

Acknowledgment. Supported by the National Institutes of Health (Grant GM33883). We thank Professor G. Czapski for sending us a preprint of ref 46 and Dr. D. Church for his help with the ESR experiments.

Registry No. $HLFe^{II}$ (HL = nta), 68391-67-3; $HLFe^{II}$ (HL = edda), 94701-47-0; H_2O_2, 7722-84-1; HCO_2^-, 71-47-6.

(43) Klaening, U. K.; Sehested, K.; Holcman, J. *J. Phys. Chem.* **1985**, *89*, 760–763.
(44) Groves, J. T.; Watanabe, Y. *J. Am. Chem. Soc.* **1986**, *108*, 7836.
(45) Aruoma, O. I.; Grootveld, M.; Halliwell, B. *J. Inorg. Biochem.* **1987**, *29*, 289.
(46) Goldstein, S.; Czapski, G.; Cohen, H.; Meyerstein, D. *J. Am. Chem. Soc.* **1988**, in press.